PROCEEDINGS OF SPIE

SPIEDigitalLibrary.org/conference-proceedings-of-spie

Dark field technology for EUV and optical mask blank inspection

Qiuping Nie, David Aupperle, Alexander Tan, Bill Kalsbeck, Qiang Zhang, et al.

SPIE.

Dark Field Technology for EUV and Optical Mask Blank Inspection

Qiuping Nie*, David Aupperle, Alexander Tan, Bill Kalsbeck, Qiang Zhang, Gregg Inderhees

KLA-Tencor Corporation, One Technology Drive, Milpitas, CA, USA 95035

*Phone: 1-408-875-4273, *Email: Richard.Nie@Kla-Tencor.com

ABSTRACT

The current industry plan is for EUV Lithography (EUVL) to enter High Volume Manufacturing (HVM) in the 2019/20 timeframe at about the 16nm half-pitch node (16hp). Reticle quality and reticle defects continue to be a top industry risk. The primary reticle defect quality requirement continues to be defined as "no reticle defects causing 10% or larger CD errors on wafer".

Traditionally, mask shops and mask blank manufacturers have been using bright field confocal technology to perform mask blank qualification. However, due to more stringent defect requirements for EUV blank defects, and the difficulty in detecting and repairing any mask defects caused by a blank defect, the industry requires a new approach to detect defects to support 16 nm hp EUV manufacturing.

To meet these emerging requirements, we have developed a new dark field imaging system for photomask blank inspection. This system can be used in the blank manufacturing process to inspect the quartz blank, to inspect after film deposition, and to inspect the finished blank after resist coating. In the mask shop, the same system can be used to inspect an uncoated blank prior to resist coating, or to perform incoming inspection on a finished blank, prior to writing.

In this paper, we report on the initial results from this new system on a range of programmed defect blanks as well as production photomask blanks. Inspection results will be shown on a variety of substrates, both for EUV blanks as well as optical blanks.

Keywords: EUV, blank mask inspection, reticle inspection, particle inspection

1. INTRODUCTION

With shrinking design node and EUV insertion, mask blank quality is becoming more and more critical to mask and wafer yield. In the past years, mask shops and mask blank manufacturers have been using bright field confocal technology to inspect mask blanks. However, the traditional technology is facing challenges in many areas such as defect sensitivity, throughput, defect disposition accuracy, system cleanliness, etc.

To address these challenges and meet increasing blank inspection requirements, we developed a new mask blank inspection system (FlashScan™) using dark field laser scanning technology. The system has been tested and characterized using various KLA-Tencor conformance reticles and industry-sourced reticles, both EUV and optical to meet 16hp requirements. The testing results show sufficient sensitivity, throughput, disposition accuracy and cleanliness. In this paper, we'll discuss the technology, algorithms, performance and test results in detail.

2. DARK FIELD LASER SCANNING TECHNOLOGY

Dark field imaging technology offers higher sensitivity in comparison to the bright field imaging technology when it comes to detecting a small particle defect on a mask blank substrate with surface roughness. As illustrated in Figure 1

Photomask Technology, edited by Peter D. Buck, Emily E. Gallagher, Proc. of SPIE Vol. 10451,
104511D · © 2017 SPIE · CCC code: 0277-786X/17/$18 · doi: 10.1117/12.2281057

below, bright field imaging typically illuminates the mask near normal incidence and collects both the reflected light and the scattered light from the defect. The surface scattering, which tends to distribute more strongly in the same direction as the reflected light, is inseparable from the defect scattering and fundamentally limits the detection sensitivity. On the other hand, dark field imaging illuminates the mask obliquely and collects the defect scattering in the direction away from the reflected light where the defect scattering dominates. This optical configuration not only suppresses the surface scattering, but also allows the surface scattering and defect scattering to be separable in the angular space, hence it can greatly improve the detection sensitivity.

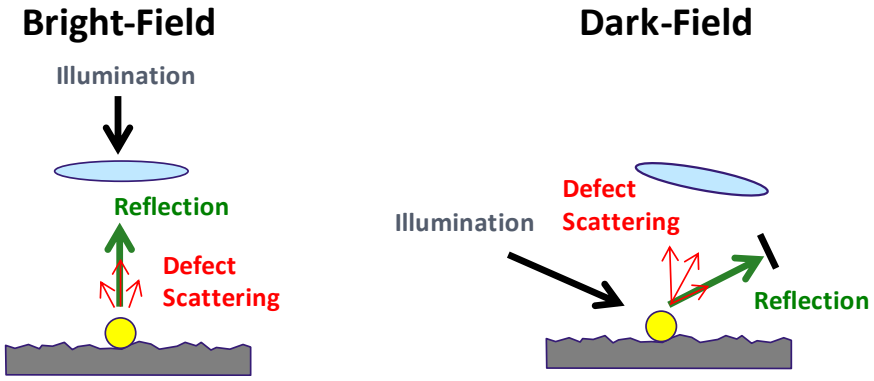

Figure 1: Illustration for bright filed versus dark field imaging

3. RESIST SENSITIVITY

Dark field imaging also offers better and more reliable sensitivity in comparison to bright field imaging for resist coated blank substrates, due to the choice of oblique illumination. Figure 2 below shows the simulated data of the scattering strength of a fixed size particle sitting on top of a resist-coated chrome blank where the resist thickness is varied. The blue and red curves are for illumination at oblique and normal incidence angles, respectively, at the same wavelength. The magnitude of the curves has been normalized by the defect scattering strength baseline when the resist thickness is set to zero, or no resist at all. In both cases, we see that the defect strength is modulated by the resist thickness variation due to the optical interference effect. However, in the case of normal incidence, the defect scattering can be strongly suppressed at certain resist thickness of interest in comparison to the baseline, leading to loss of sensitivity. In contrast, the defect scattering strength under oblique illumination holds well against the baseline, no matter what the resist thickness is, resulting in more consistent sensitivity performance.

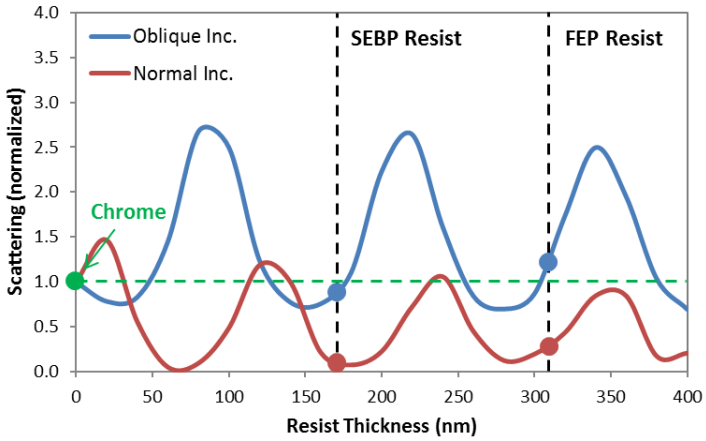

Figure 2: Scattering strength comparison between bright field and dark field systems

4. ALGORITHMS ADVANCE

FlashScan defect detection utilizes Die to Die Inspection (DDI) to inspect a blank reticle. Since both of the test and reference images are from the actual blank surface itself, the difference image may have extra noise in certain situations. To enhance defect signal and reduce noise, we developed an additional Single Die Inspection (SDI) algorithm that can run concurrently with DDI. The SDI algorithm uses the same test image as DDI but renders a much "quieter" reference image to subtract for difference image. The SDI and DDI were compared using same inspection condition on various FlashScan test masks.

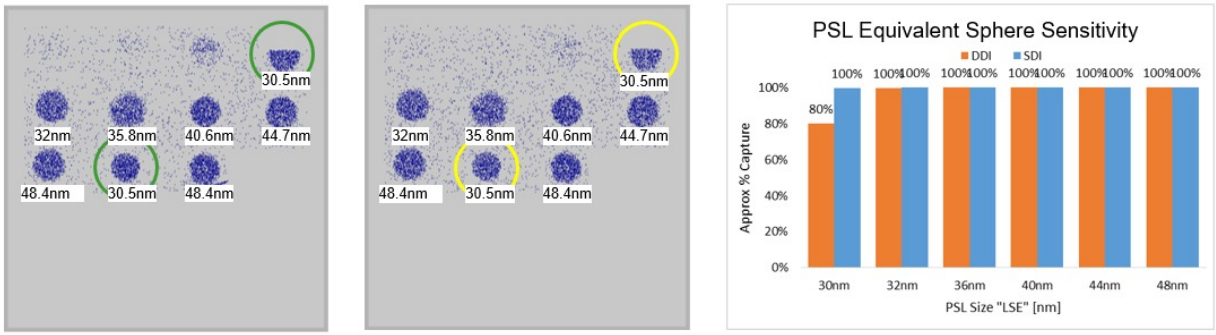

Figure 3: Inspection results comparison for SDI and DDI algorithms

Figure 3 shows the inspection results from SDI and DDI algorithms on FlashScan OMOG test mask. The test mask was manufactured with particle depositions ranging from 30nm to 48nm in size across the mask. In the capture rate comparison chart, the blue bar represents the SDI capture rate that shows 100% capture for particles down to 30nm in size. The orange bar represents the DDI capture rate that shows 80% capture for particles down to 30nm in size. The result comparison shows the performance benefit of SDI algorithm improvement.

5. PATTERN CAPABILITY

One key use case for blank inspection systems is to inspect process monitor masks. It requires inspection system to handle simple 1D or even 2D patterns during an inspection. FlashScan utilizes dark field laser scanning technology, it can handle simple 1D pattern by a natural filter. For 2D pattern filter, FlashScan utilizes proprietary hard aperture Fourier Filter (FF). During the image processing, we apply Fourier transformation to a patch image and use Fourier Filter to remove peaks that are caused by repeating pattern from an image (Figure 4-1) then reconstruct the image with the repeating pattern removed.

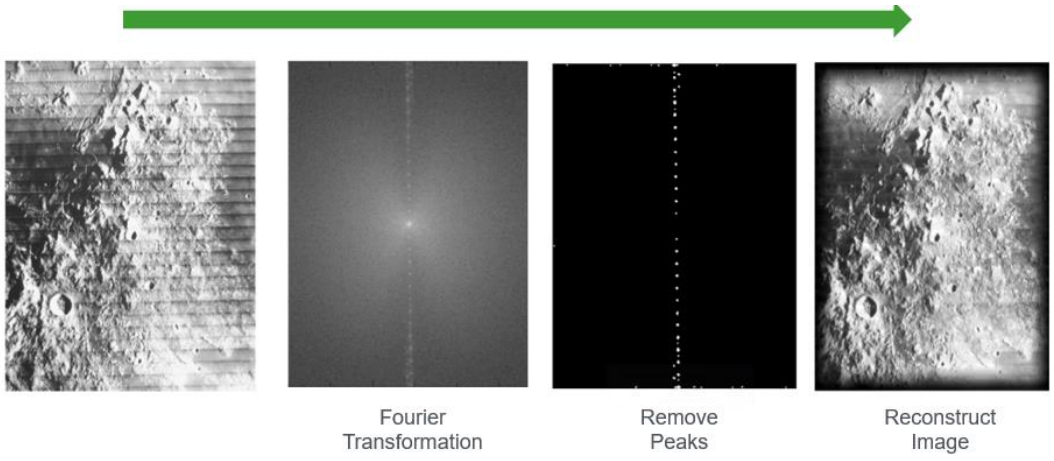

Figure 4-1: Illustration of Fourier Filter to reduce repeating pattern [1]

Figure 4-2 shows defect signal comparison from a 2D process monitor mask. The background pattern of this monitor mask contains both 1D and 2D patterns with variable pitch and pattern discontinuities. On the left is defect signal from three channels on FlashScan with FF enabled. On the right is same defect's signal from three channels without FF. The comparison shows that FF can completely remove the background 2D filter, and thus extract defect signal and suppress background noise. The increased SNR is critical to detect defects for process monitor purpose. We were able to inspect an entire monitor mask with one inspection and detect 276 defects.

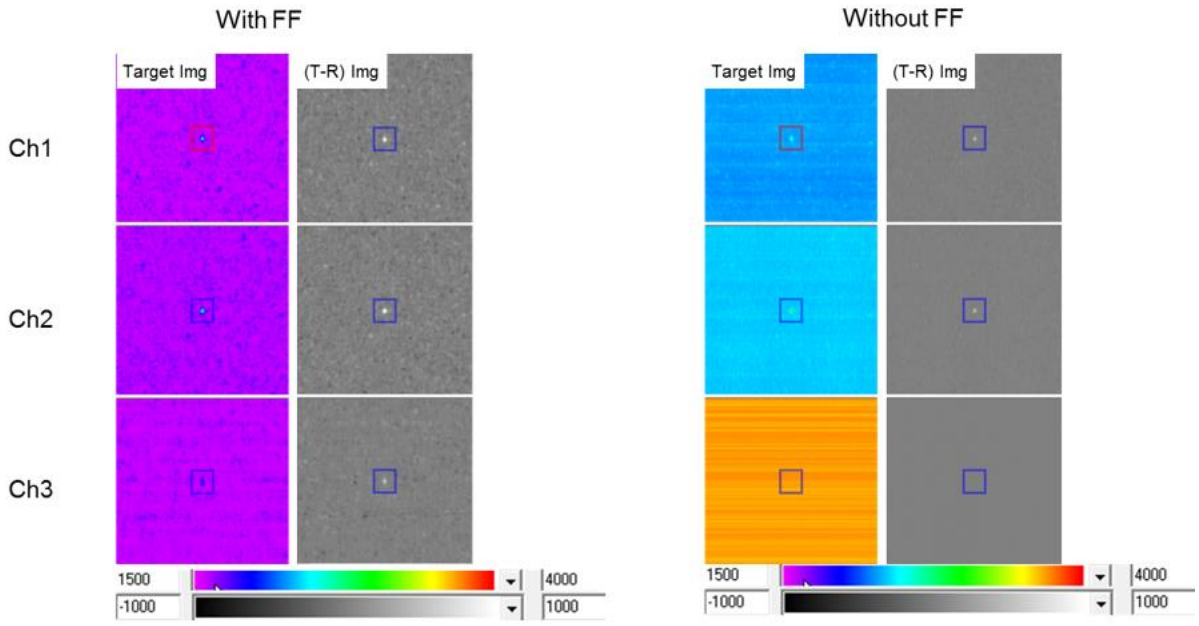

Figure 4-2: Defect signal and noise comparison with or without Fourier Filter

6. DEFECT CLASSIFICATION

One of the architectural advantages for FlashScan is the 3 detection channels. Images from 3 channels not only enhance defect detection sensitivity, they also provide extra information for defect disposition. Based on our study, different defect type has different scattering signatures in the 3 channels. For defects with height, such as particles or bumps, the normal channel has weaker signal compared with side channels. For defects with depth, such as pits or pinholes, the normal channel has stronger signal compared with side channels. We introduced "TopRatio" parameter, defined below, to characterize this behavior and apply it for defect classification.

$$\boldsymbol{TopRatio} = \frac{\boldsymbol{Min\ Energy\ (Ch1,\ Ch2)}}{\boldsymbol{Energy\ Ch3}}$$

Figure 5 shows defect classification result that distinguish pin hole versus particles. 100nm pin hole defect have "TopRatio" value no more than 1.5, whereas 50nm particles have "TopRatio" greater than 2. The distinct separation suggests good classification potential of FlashScan using "TopRatio".

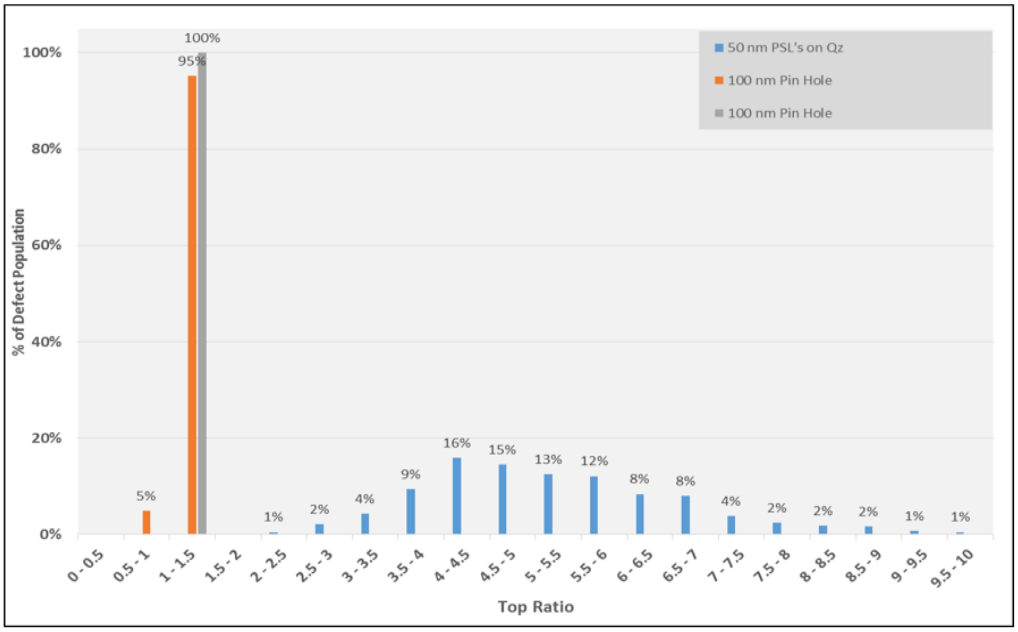

Figure 5: Defect classification result using TopRatio

7. DEFECT SIZING

For the blank inspection use case in mask production, it is important to not only detect a defect but also provide sizing information of a defect. The sizing information will be used to determine the next process steps for the blank. Without an accurate sizing solution, a user needs to review all defects from a SEM tool, which increases the cycle time of mask production.

To meet the sizing requirement for blank inspection, we developed a combined solution that utilizes the patch image and a review camera image for different defect size categories. Two Program Defect Mask (PDM) were tested and the results show good accuracy between FlashScan measured size versus programmed size.

Figure 6-1 shows sizing result for a Cr pin dot PDM. This PDM has program defect size ranging from 28nm to 1980nm. The FlashScan reported size shows +/- 20% accuracy compare with programmed size for defects below 150nm and +/- 15% accuracy for defect above 150nm.

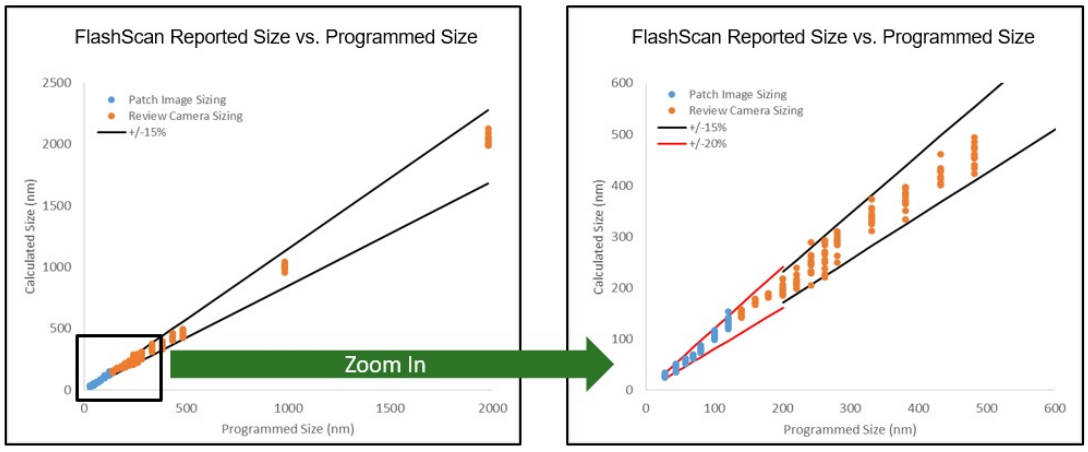

Figure 6-1: Defect sizing result for a Cr pin dot program defect mask

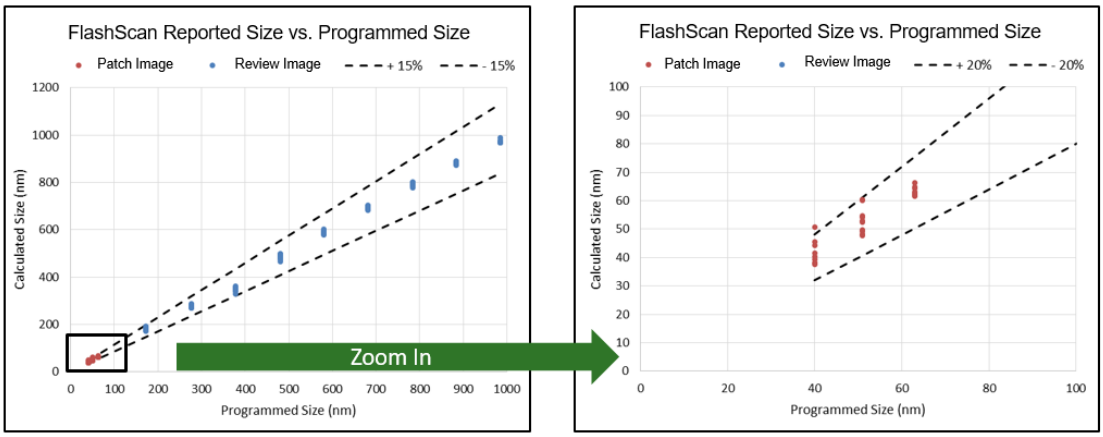

Figure 6-2: Defect sizing result for a resist coated pin hole program defect mask

Another resist coated pin hole PDM with defect size range between 40nm to 1000nm was also tested (Figure 6-2). The FlashScan reported size shows +/- 20% accuracy compare with programmed size for defects below 150nm and +/- 15% accuracy for defect above 150nm. Both result suggests good sizing capability from FlashScan.

8. EUV SENSITIVITY

One key advantage for FlashScan is sensitivity on EUV reticles. We tested a variety of EUV reticles including EUV blanks with natural defects and EUV reticles with programmed defects from industry sources.

Figure 7-1 shows the performance on a customer EUV Absorber blank mask. FlashScan demonstrated detection down to 30nm based on customer provided sizing.

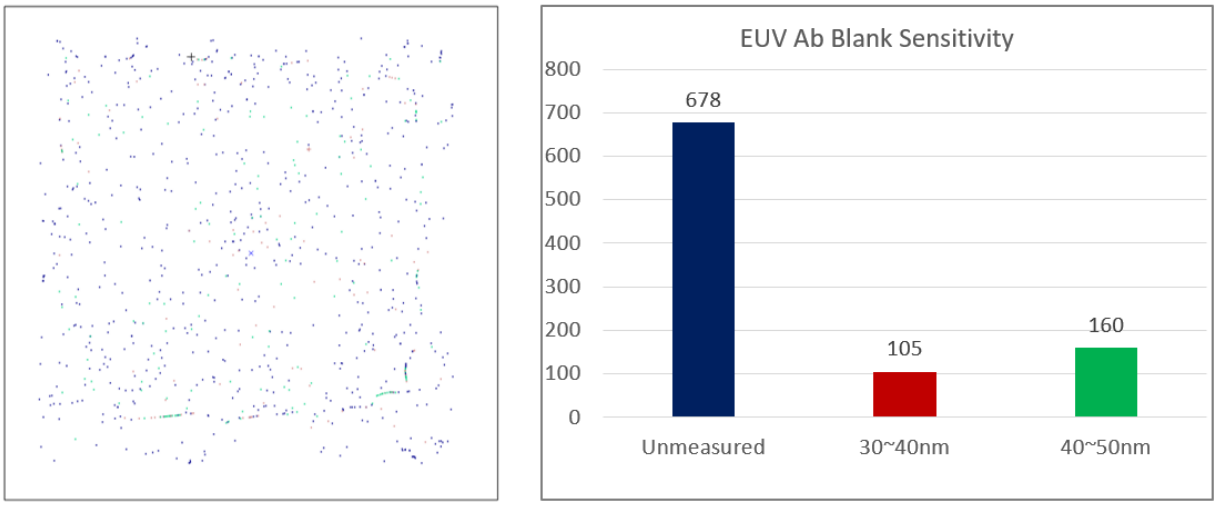

Figure 7-1: FlashScan sensitivity on EUV absorber blank

Figure 7-2 shows the performance on a customer EUV programmed pin hole defect mask. The largest defect for each inspection area is located at the lower left corner of the array. In the 100nmx100nm to 10nmx10nm defect size region, for example, the defect at lower left corner is programmed to be 100nmx100nm in size. Moving in the X direction, the defect width decreases by 5nm in each step. Moving in the Y direction, the defect height decreases by 5nm in each step. Therefore, the smallest defect in the array located at the upper right corner, is programmed to be 10nm by 10nm.

Although there's uncertainty in pin hole etch performance, FlashScan demonstrated a detection down to 35nm by 35nm according to programmed size.

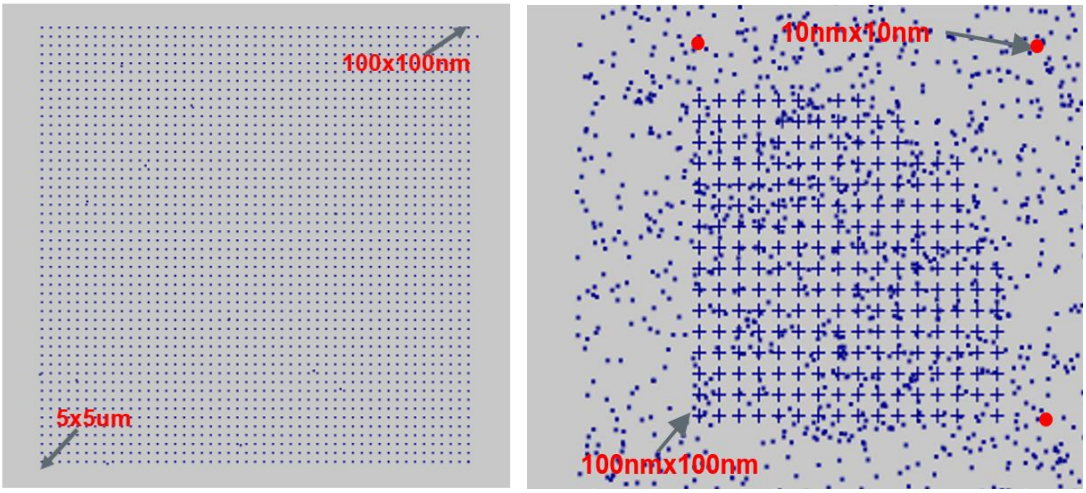

Figure 7-2: FlashScan sensitivity on programmed pin hole defect mask

9. EUV LEVEL CLEANLINESS

With shrinking mask designs and upcoming EUV insertion, even very small defects on reticle may cause a printing impact on wafer. It is important that the interior of the inspection system be exceptionally clean, and the handling is done according to EUV standards. The FlashScan 2xx accomplishes this need with careful design of the reticle handling and throughout the entire system. One example is the design of the reticle chuck, which was developed to minimize the contact area of the entire mask front side and back side (See Figure 8). There are two additional benefits achieved through the design: EUV reticle backside inspection with or without pellicle and reticle backside inspection with resist coated front side.

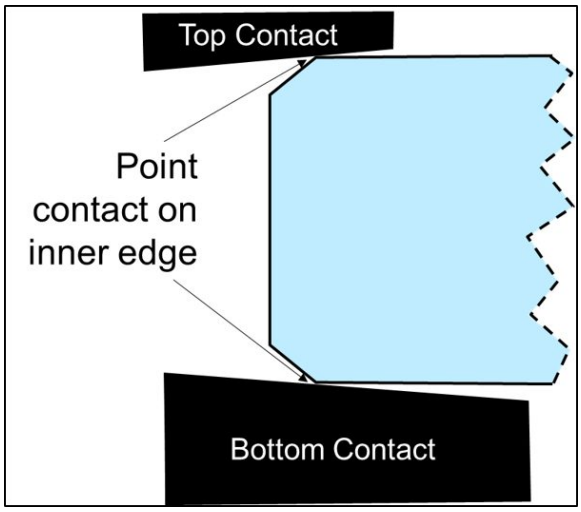

Figure 8: FlashScan reticle handling illustration

A common cleanliness test is to cycle a test reticle through multiple load and unload cycles. Then inspect the cycled mask to determine the adder count and size. The design target for the FlashScan 2xx is to meet EUV level cleanliness

requirements – not adding more than 1 particle greater than 35nm in size through 20 load and unload cycles. Tests using at least 20 load and unload cycles have been performed on multiple FlashScan 2xx systems and the results are passing EUV level cleanliness requirements.

10. CONCLUSION

We have discussed the capabilities of FlashScan system for both optical and EUV mask blank inspection. FlashScan shows very good performance on defect sensitivity, defect dispositioning, system cleanliness, and pattern handling.

We believe these capabilities will be critical to support EUV and optical mask manufacturing for upcoming L7 and L5 design nodes.

11. FUTURE WORK

We expect to receive more industry EUV blanks for upcoming L7 and L5 design nodes. We plan to test the FlashScan system with these blanks and identify areas for further improvement. We also expect to receive more after write and after develop reticles for AWI and ADI inspection.

ACKNOWLEDGEMENTS

The authors thank the FlashScan product development team and industry sources for EUV/Optical test reticles that contributed to the development and testing of the FlashScan system.

REFERENCES

[1] Zisserman, A. Lecture 2: 2D Fourier transforms and applications. Retrieved from http://www.robots.ox.ac.uk/~az/lectures/ia/lect2.pdf